

Identification of New Potent GPR119 Agonists by Combining Virtual Screening and Combinatorial Chemistry

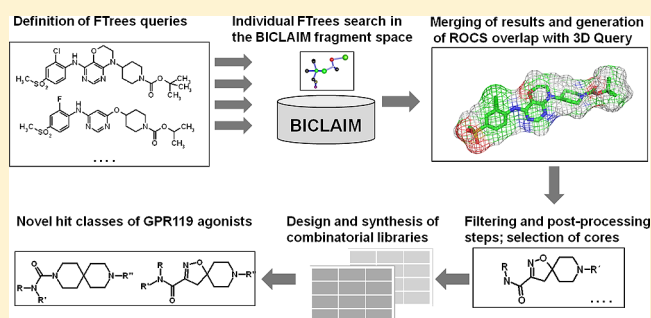
Bernd Wellenzohn,[†] Uta Lessel,[†] Andreas Beller,[‡] Timo Isambert,[§] Christoph Hoenke,[‡] and Bernd Nosse^{*,§}

[†]Research Germany/Lead Identification and Optimization Support, Boehringer Ingelheim Pharma GmbH & Co. KG, Birkendorfer Straße 65, 88397 Biberach an der Riss, Germany

[‡]Research Germany/Medicinal Chemistry/Combinatorial Chemistry, Boehringer Ingelheim Pharma GmbH & Co. KG, Birkendorfer Straße 65, 88397 Biberach an der Riss, Germany

[§]Research Germany/Medicinal Chemistry, Boehringer Ingelheim Pharma GmbH & Co. KG, Birkendorfer Straße 65, 88397 Biberach an der Riss, Germany

ABSTRACT: Virtual screening in a huge collection of virtual combinatorial libraries has led to the identification of two new structural classes of GPR119 agonists with submicromolar in vitro potencies. Herein, we describe the virtual screening process involving feature trees fragment space searches followed by a 3D postprocessing step. The in silico findings were then filtered and prioritized, and finally, combinatorial libraries of target molecules were synthesized. Furthermore the so-called “activity-anchor principle” is introduced as an element to increase the chance to generate true hits. An activity anchor is a structural element expected to provide key contributions to a certain biological activity. Application of this technique has led to the discovery of two new GPR119-agonist hit series, one of which was further optimized to progress as a novel lead class.



INTRODUCTION

In the year 2000 at least 171 million people in the world suffered from type 2 diabetes mellitus (T2DM), and it is expected that the incidence of this disease will almost double within just one generation to reach 335 million in 2025.¹ Consequently there is an enormous need for innovative drugs in this field. A characteristic feature of the progression of T2DM is a gradual loss of pancreatic β -cell function.² The G-protein-coupled receptor GPR119 was recently deorphanized³ and is a focus of current drug development as a new antidiabetic target.^{4–7} The receptor is expressed in pancreatic β -cells as well as in the gastrointestinal tract,⁷ and GPR119 agonists have been shown to promote the glucose dependent insulin secretion.⁵ Furthermore it has been reported that GPR119 agonists stimulate the secretion of glucagon-like peptide 1 (GLP-1) from intestinal L-cells.⁵ GPR119 agonists support a very interesting new drug concept, as they are expected to regulate the glucose homeostasis by different mechanisms. Several GPR119 agonists have been published, and some compounds have already reached the stage of clinical trials.^{8–13}

In our group, similarity searches in a huge virtual library have been performed in addition to high-throughput screening (HTS) with the aim to identify new GPR119 agonists. Our virtual library called BICLAIM (Boehringer Ingelheim Comprehensive Library of Accessible Innovative Molecules)

has already been published¹⁴ and is similar to a database reported by Pfizer.¹⁵ BICLAIM is based on combinatorial reactions and stored in a feature trees (FTrees) fragment space. When the virtual screening (VS) campaign for GPR119 agonists was performed, the virtual chemical space contained about 1600 scaffolds and 30 000 reagents encoding about 5×10^{11} theoretically chemically accessible molecules. Our continuous efforts to expand the BICLAIM space by extracting in-house and external (data) sources have led to approximately 41 300 scaffolds today. For each library scaffold, possible synthesis routes and lists of reagents compatible with the corresponding chemistry providing the decoration of the cores have been collected and stored.

The advantage of concentrating on combinatorially accessible space is that this chemistry is usually very robust and fast. Thus, interesting virtual hits can be easily synthesized and explored by combinatorial chemistry. We rely on synthetic chemistry which is well established preferably in-house or in literature as well as on readily available building blocks for our combinatorial chemistry efforts to ensure fast alignment with other hit identification activities (e.g., HTS or fragment based screening, FBS). Although the VS techniques enrich active molecules in the hit set, very similar molecules have a problem of inaccurate

Received: October 23, 2012

Published: December 4, 2012

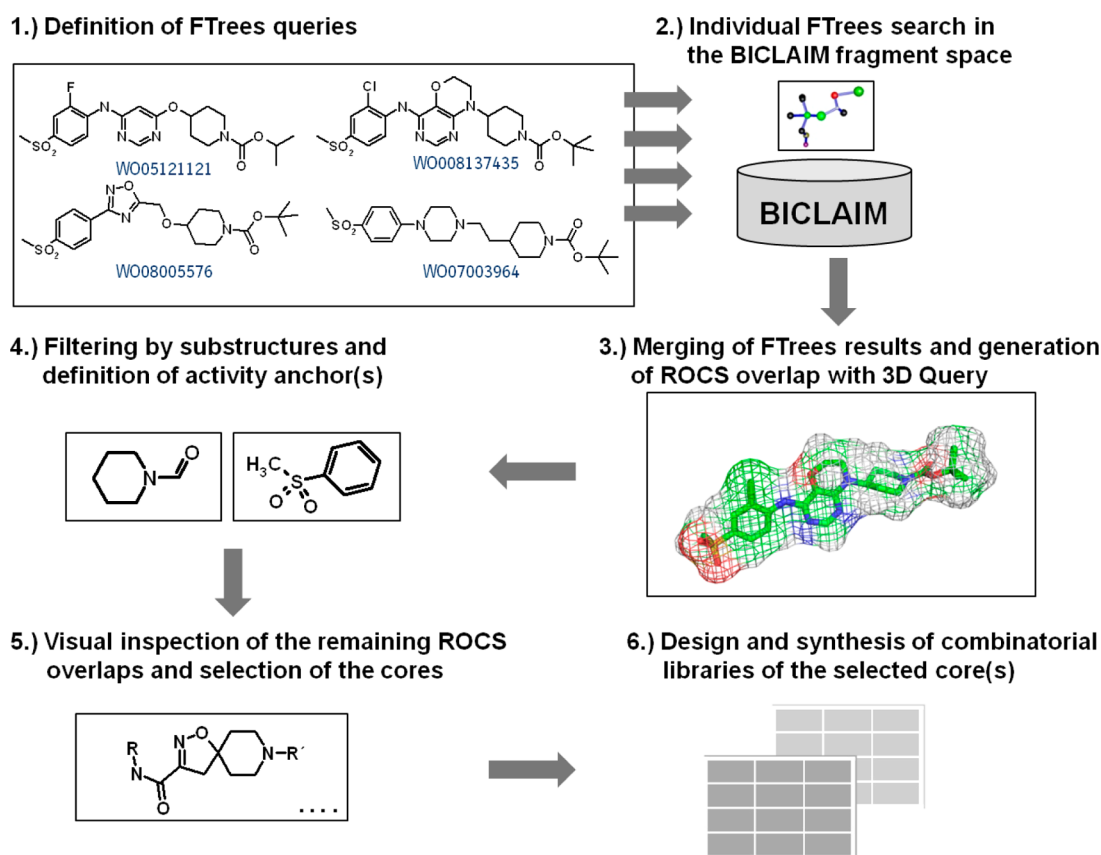


Figure 1. Workflow of FTrees fragment space searches at Boehringer Ingelheim (BICLAIM campaign).

predictivity of their biological activity in virtual screening and there is no inherent solution to avoid false positives. Therefore, it is not recommended to synthesize and test exclusively the few best predicted molecule(s) but a larger number of analogues in a combinatorial library. This enhances the chance to get active hits and additionally allows for a fast assessment of structure–activity-relationships (SARs). The SAR information obtained in the first generation of molecules can be used for the design of follow-up libraries during an exploration and/or optimization phase. In our hands the combination of virtual screening and combinatorial chemistry has been very successful in identifying new lead structures for several projects. Here we describe the application of this technique for the discovery of new GPR119 agonists. Two new classes with submicromolar *in vitro* potency could be identified.

RESULTS AND DISCUSSION

Virtual Screening. The outline of the BICLAIM workflow is illustrated in Figure 1.

The virtual library BICLAIM is stored in a FTrees fragment space which allows for fast similarity searches against given queries based on the FTrees descriptors.^{16–18} The FTrees software cleaves all rotatable single bonds and represents the resulting fragments by nodes that are connected in the same manner like the fragments. Each node is annotated with steric properties of the corresponding fragments like for instance its volume and an interaction profile with the H-bond donor and acceptor capabilities.¹⁶ In order to compare two molecules based on FTrees descriptors, a FTrees score describing the similarity of the properties of the corresponding nodes is maximized. This involves a conformation independent

comparison of the nodes' topologies. The fragment space module¹⁸ of the FTrees software is making use of the additivity of the FTrees similarity and thus allows searching a large virtual (combinatorial) space. This approach is very fast, as only the fragments representing the potential parts of a molecule from combinatorial chemistry have to be considered instead of comparing enumerated molecules.

The resulting hits are then prioritized by a project-specific postprocessing workflow (steps 3 and 4 in Figure 1). As a consequence, interesting similar molecules containing all essential pharmacophoric features can be successfully identified by FTrees fragment space searches, but the method does not guarantee an optimal arrangement in space. We postprocess the FTrees results by 3D virtual screening techniques like docking or 3D alignments to filter and identify those hits that are also similar to the query molecules in 3D (see step 3 in Figure 1). Finally, the summarized results are visually inspected by a team of medicinal, computational, and combinatorial chemists with the goal to select the most promising cores (step 5 in Figure 1). The next step benefits from the fragment space being based on combinatorial chemistry. Instead of synthesizing only the few “optimal” FTrees hits, we design and synthesize combinatorial libraries usually comprising 50–1000 compounds. In many cases we observed that the decoration that is suggested by *in silico* methods to be optimal for the query molecules indeed resulted in active hits. However, these hits usually need further optimization, e.g., by improved decoration of the core or slightly modified scaffolds in order to reach optimal activity.

For the design of focused combinatorial libraries different options can be used. We apply the software tool LoFT which has been developed for the design of focused combinatorial

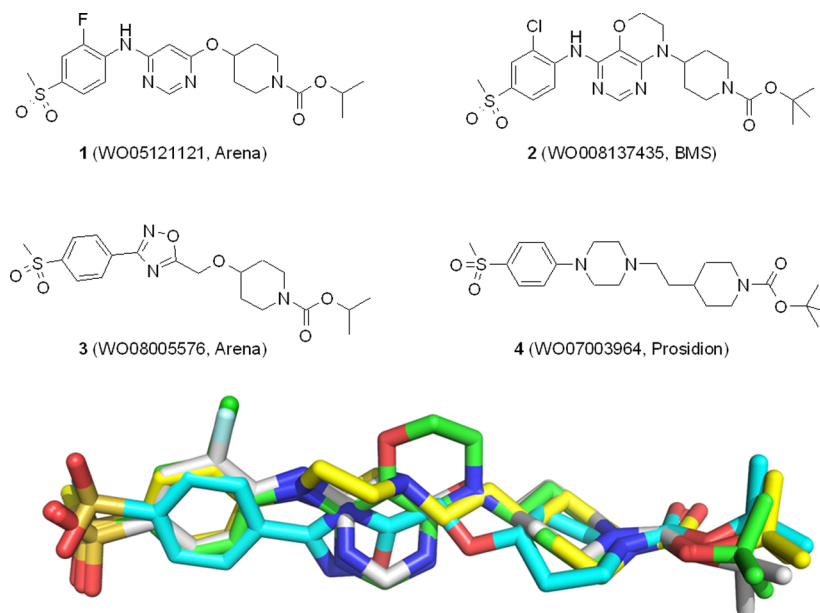


Figure 2. Query molecules and their superimposition (1 white, 2 green, 3 blue, 4 yellow).

libraries based on feature trees similarity and physicochemical properties.^{19–21} However, for the application in the GPR119 project we concentrated on gaining agonistic activity by taking only the similarity to queries 1–4 into account and did not consider any physicochemical properties for reagent selection. It is also possible to enumerate virtual libraries according to the reaction scheme and to select the most appropriate reagents based on an assessment of the products, e.g., by looking at docking or 3D alignment results. Last but not least we have found it useful to manually enrich the *in silico* selected reagents by making use of SAR information or other project specific knowledge. In any case an extensive manual interaction driven by the experience of the project team is usually included to finalize the decoration of a core.

In addition to standard BICLAIM campaigns in which usually not much is known about the binding mode or SAR contributions of the query molecules, we have also introduced the so-called “activity anchor principle”. In our hands an activity anchor is a structural element known to or at least supposed to provide key contributions to a certain biological activity. Usually the activity anchor is defined by analyzing the SAR of the query ligands and literature or in-house information. The presence or absence of an activity anchor or the option to introduce the corresponding structural feature via the synthesis protocol can be used to filter the hit lists for core selection (step 4 in Figure 1). Furthermore the activity anchor could itself serve as a core which (by applying suitable chemistry) can be decorated by means of focused two-dimensional combinatorial libraries. Alternatively, scaffold replacement tools like CAVEAT,²² ReCore²³ or the scaffold replacement and ligand growing tools implemented in MOE²⁴ can also be applied to further elaborate activity anchors. This “activity anchor principle” is widely used in Boehringer Ingelheim’s BICLAIM campaigns. A recent analysis of several projects showed that using an activity anchor doubles the chance of identifying true hits in a BICLAIM virtual screening campaign.

BICLAIM Virtual Screening and Synthesis Campaigns.

At the time at which the in-house virtual screening campaign for GPR119 agonists was initiated, a wealth of different agonists

was already described in the literature and in patent applications. Four structurally different known GPR119 agonists were selected as query molecules (see Figure 2).^{25–29} These compounds differ mainly in the central part but display a similar left-hand and right-hand side decoration pattern. They all share a methyl sulfone substituted aryl part on the left-hand side as well as an alkyl carbamate on the other side. On the basis of the hypothesis that these peripheral moieties are important for the activity, these features were chosen as “activity anchors”.

The FTrees fragment space search in BICLAIM provided thousands of virtual hits per query. Usually each hit list has to run through a postprocessing step on its own, but in this case all query molecules overlapped well in 3D, although they were coming from different structural classes.

This 3D overlap indicates that they probably all share an identical binding epitope, which allowed us to combine all the hits from different queries into one large hit list. For each query molecule the most similar 10 000 FTrees hits were kept for postprocessing.

In this case 3D alignments of the virtual hits were generated with ROCS.²⁹ As the respective query, we chose compound 2 because of its relatively high rigidity. The putative active 3D conformation of 2 was defined based on the overlap with the other three queries, as shown in Figure 2. The FTrees hits were prepared for the ROCS alignments by applying Corina³⁰ and Omega.³¹ Recently, the first pharmacophore model for GPR119 agonists was published.³² However, at the time this work was conducted, the pharmacophore model was not available, and thus, this information could not be included in our postprocessing analysis. The ROCS alignments were visually inspected making use of the MOE mdb-browser functionality²⁴ to select the most promising scaffolds. In this case the main focus was on molecules carrying both activity anchors. From these molecules two cores were selected for synthesis campaigns.

The first virtual hit class that was selected for synthesis in combinatorial chemistry consisted of a 3,9-diaza-spiro[5.5]-undecane core (see 5, Figure 3). Both activity anchors

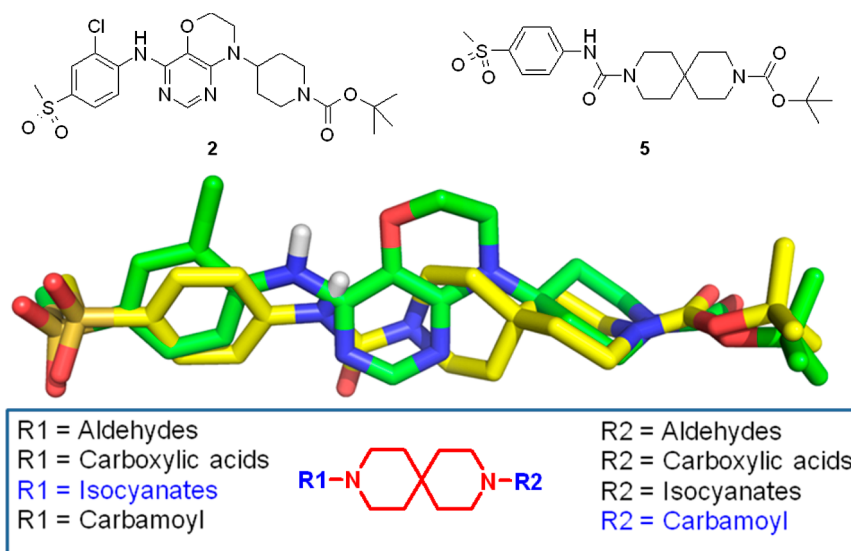


Figure 3. ROCS²⁹ overlap of query 2 (green) with spiro compound 5 (yellow), general information on the core and its possible decoration as stored in BICLAIM.

Scheme 1. Synthesis of Spiro Ureas 9a–c (Library 1)

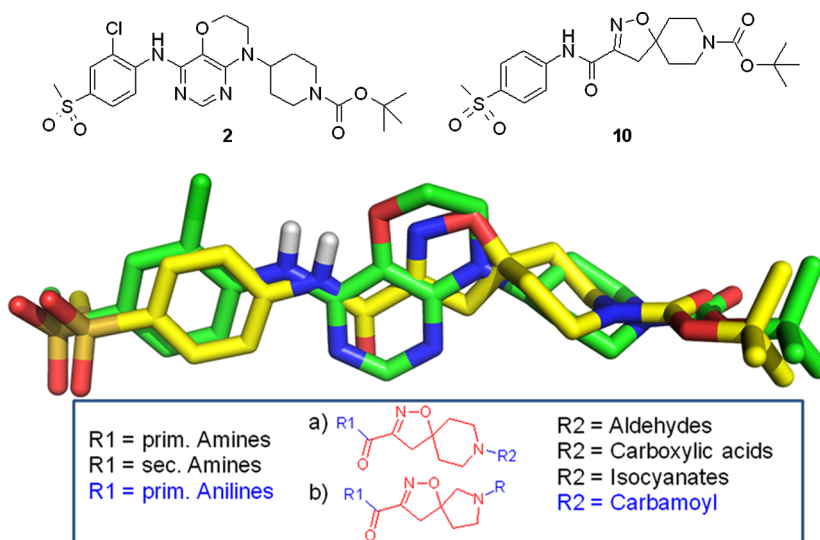
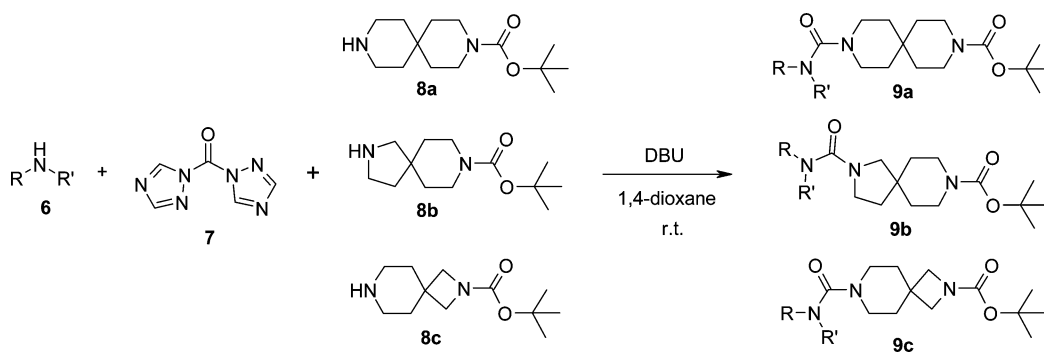


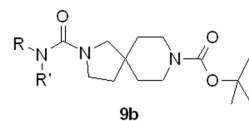
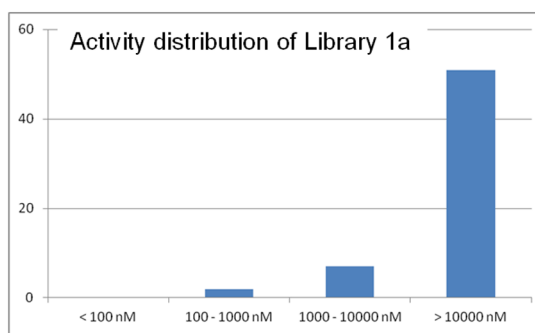
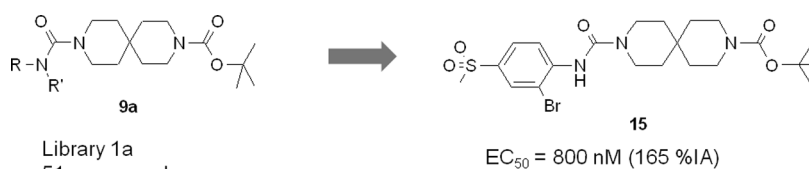
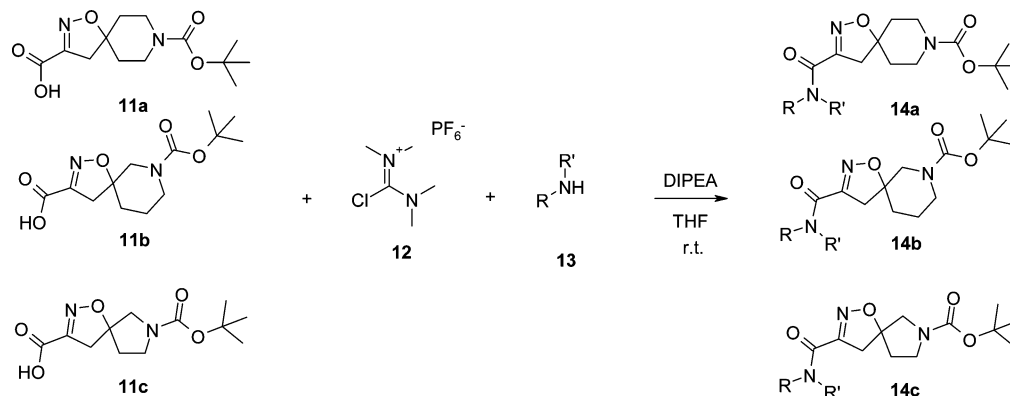
Figure 4. ROCS²⁹ overlap of query 2 (green) with spiro compound 10 (yellow), the general information on the core and its possible decoration as stored in BICLAIM.

superimpose very well, whereas the spirocyclic core (yellow) does not match optimally with the steric demand of the central part of query 2 (green). However, we assumed that the core only arranges the activity anchors correctly in space and

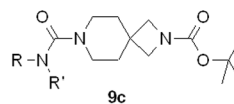
provides the right distance between the aryl and the carbamate moiety and should itself not contribute too much to binding.

The suggested chemistry to address the left-hand side (LHS) decoration involved reductive amination with aldehydes, amide

Scheme 2. Synthesis of Spiro Dihydroisoxazoles 14a–c (Library 2)



Library 1b
55 compounds
all EC₅₀'s > 10,000 nM



Library 1c
56 compounds
all EC₅₀'s > 10,000 nM

Figure 5. Outcome and activity distribution of library 1.

bond formation with carboxylic acids, carbamate synthesis with carbamoyl halides, and finally urea formations with isocyanates. Proposed variations for the right-hand side (RHS) were analogous; however, we concentrated on alkyl carbamates that were similar to the query decoration (cf. the activity anchor principle). The urea linker between core and aryl moiety provided the best superimposition with the queries and was therefore chosen for our initial synthesis campaign. According to the activity anchor principle, we maintained a *tert*-butyl carbamate on the right-hand side and varied the core as well as the aryl part of the urea in a combinatorial library matrix. In order to diversify the core with respect to orientation and absolute length, not only 3,9-diaza-spiro[5.5]undecane core **8a** but also the cores 2,8-diaza-spiro[4.5]decane **8b** and 2,7-diaza-spiro[3.5]nonane **8c** were employed (see Scheme 1). Because of limited accessibility of isocyanates with the appropriate decoration, we synthesized the targeted ureas using amines from our in-house amine collection and a suitable coupling reagent. During method development in order to optimize the

reaction conditions, we found that 1-1'-carbonyldi(1,2,4-triazole) (**7**, CDT) was superior to other coupling reagents like *N,N'*-carbonyldiimidazole (CDI) or 4-nitrophenyl chloroformate.

The synthesis (Scheme 1) involved preactivation of 72 amines/anilines **6** with CDT and addition of the corresponding readily available spiro compounds **8a–c** on a 0.1 mmol scale. 1,4-Dioxane as a solvent and 1,8-diazabicyclo[5.4.0]undec-7-ene (DBU) as a base showed the best conversions throughout the differently reactive amines used. The crude products were subsequently purified by automated preparative reversed phase HPLC using narrow gradients. Yields were generally good, varying between 20% and 90%, and a total number of 194 (out of 216) compounds were submitted for in vitro testing for GPR119 agonistic activity.

The second class of interesting virtual hits that was selected for synthesis consisted of an alternative spirocyclic system (1-oxa-2,8-diaza-spiro[4.5]dec-2-ene **10**). The core, when properly decorated, overlaps very well with the query molecule (see

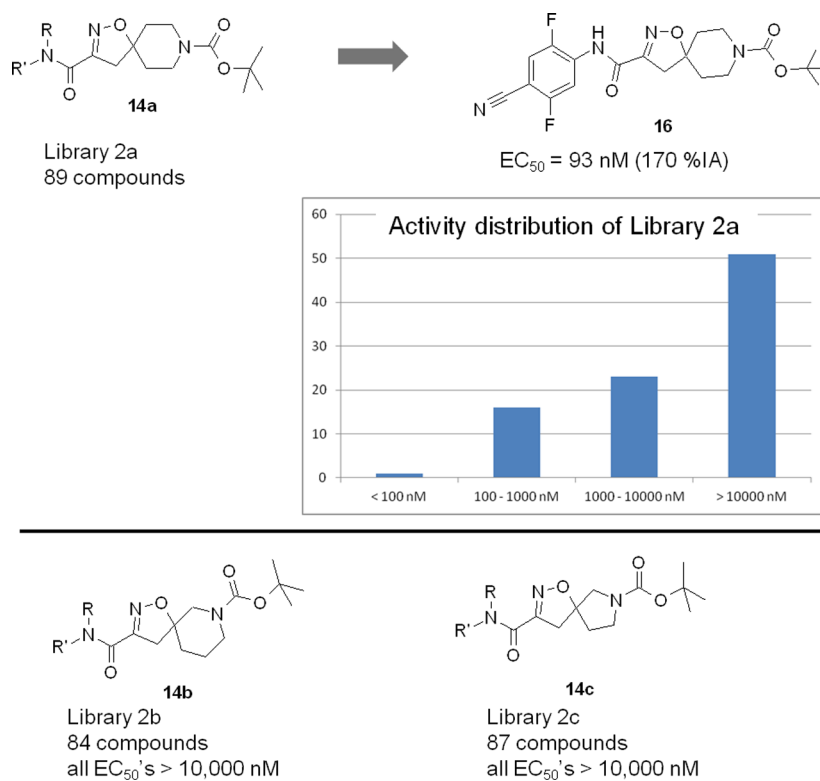


Figure 6. Outcome and activity distribution of library 2.

Figure 4). The spirocyclic system again allows the incorporation of both activity anchors and arranges them optimally in the 3D space. Core 10 represents a very rigid system that we expected not to lose too much conformational entropy upon binding. Although the overlap appears obvious retrospectively, the idea of using spirocyclic cores had so far not been in the focus of our medicinal chemistry activities for GPR119 agonists.

Similar to the first library (vide supra) we decided to keep the RHS carbamate moiety constant as an activity anchor while varying the amines for the amide bond formation and simultaneously also varying the core as depicted in Scheme 2. The selection of amines was primarily based on an acceptable superimposition with queries 1–4 and by taking into account published and in-house SAR knowledge. Therefore, we focused on primary (het)arylamines decorated with diverse substituents. The 6-ring spiro-dihydroisoxazole 11a (see Scheme 2) gave proper superimpositions with the queries; however, its pyrrolidine 5-ring analogue (see 11c) was also found interesting. The 3-piperidino analogue of 11a, 11b was additionally included in order to diversify the structural space. Method development prior to library synthesis showed that N,N,N',N' -tetramethylchloroformamidinium hexafluorophosphate (TCFH, 12) gave the best conversions with respect to the broad reactivity spectrum of the employed amines compared to other coupling reagents like Mukaiyama's reagent (2-chloro-1-methylpyridinium iodide), TBTU, or its aza-analogue HATU.³³

The library (three carboxylic acids 11a–c combined with 95 different alkyl- and (het)arylamines 13) was synthesized on a 0.1 mmol scale using TCFH (12) to preactivate the carboxylic acid followed by addition of the corresponding amine 13 and purification by means of automated preparative reversed phase HPLC (narrow gradients). 261 of theoretically 285 compounds

were obtained in generally acceptable to good yields ranging between 10% and 88%.

Biological Results and Hit Optimization. All synthesized compounds were tested for their agonistic activity (potency as EC_{50}) and their efficacy (intrinsic activity, % IA) toward the human GPR119 receptor using an ALPHAscreen cAMP assay. In this assay, the intrinsic activity as stimulation of the receptor is reported in %, the relative activity of the test compounds being compared to the efficacy of N -(4-methanesulfonylphenyl)-5-nitro-6-[4-(phenylsulfonyl)piperidin-1-yl]pyrimidin-4-amine,³⁴ which was set to 200%. We regarded compounds exceeding 160% IA stimulation as full agonists, whereas compounds between 130% IA and 160% IA were considered as partial agonists.

The outcome of the activity distribution of the initial in vitro testing toward activity on human GPR119 receptors of compounds derived from library 1 is depicted in Figure 5.

Overall we obtained disappointing results, as only ureas of a 3,9-diaza-spiro[5.5]undecane-type core (see 9a in library 1a) yielded active compounds, albeit with only modest potency. The most active derivative was 15, displaying an EC_{50} of 800 ± 260 nM, a full agonist with an intrinsic activation of $165 \pm 9\%$ IA. However, the structure–activity relationships were rather steep, which did not encourage us to invest in further syntheses.

Biological in vitro results for library 2 also showed a steep SAR, again with a strong preference for one specific core variation (see Figure 6). All synthesized 1-oxa-2,7-diaza-spiro[4.5]dec-2-enes (see 14b in library 2b) or 1-oxa-2,7-diaza-spiro[4.4]non-2-enes (see 14c in library 2c) were inactive. However, we were pleased to discover that some compounds of type 14a (see library 2a) displayed submicromolar potencies. The most active compound was 16 with an EC_{50} of 93 ± 48 nM showing full agonistic activity of $170 \pm 10\%$ IA.

The vast differences in potency could not be explained solely by the quality of the overlap compared to the queries, as all molecules gave acceptable superimpositions. Especially when it comes to small structural variations, computational methods may not always sufficiently predict their influence. On the basis of these promising results, we initiated a hit-to-lead approach in order to further improve the potency and other *in vitro* parameters (data not shown). Structural modifications involved combinatorial variations of the LHS arylamine moiety which were closely related to the difluoro-*p*-cyano substitution pattern of **16**. Also, we diversified the carbamate portion by introducing further alkyl substituents but also included bioisosters and other known binding motifs (see Figure 7).³⁵

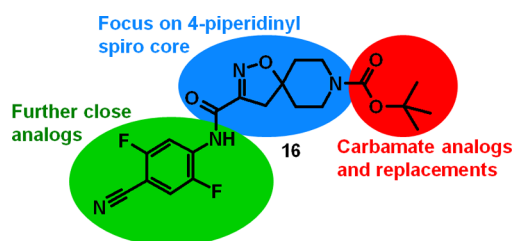
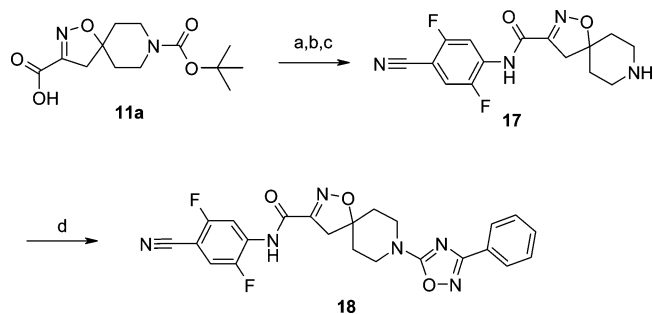


Figure 7. From hit to lead: strategies for structural modification of **16**.

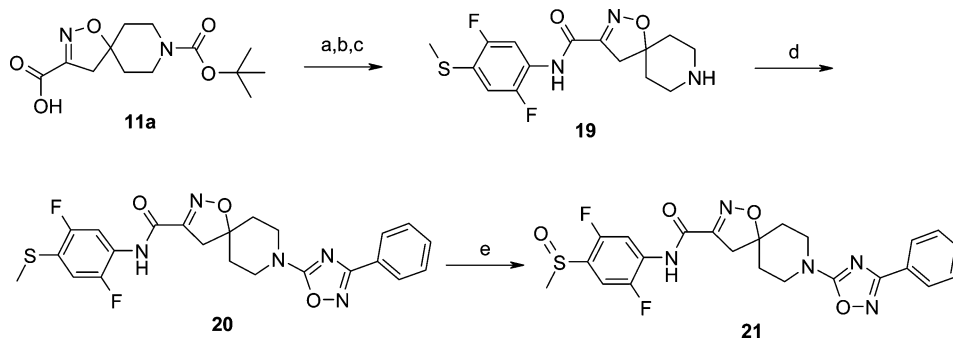
Scheme 3. Synthesis of Oxadiazole **18**^a



^a(a) TCFH, DIPEA, DCM, r.t.; (b) 4-amino-2,5-difluoro-benzonitrile; (c) dichloromethane, TFA, 43% (over three steps); (d) 5-chloro-3-phenyl-[1,2,4]oxadiazole, DIPEA, NMP, 160 °C, 50%.

4-(Pyrimidin-2-yl) substituents and 3-alkyl-1,2,4-oxadiazoles attached to the nitrogen of the piperidine can be found in recent patent literature as replacements for the carbamate part.^{36,37} Therefore, compound **18** was synthesized as outlined

Scheme 4. Synthesis of Spiro-Compound **21**^a



^a(a) HATU, DIPEA, dichloroethane, r.t.; (b) 2,5-difluoro-4-methylsulfanyl-phenyl amine; (c) HCl in diethyl ether, 44% (over three steps); (d) 5-chloro-3-phenyl-[1,2,4]oxadiazole, DIPEA, NMP, 150 °C, 51%; (e) 3-chloroperoxybenzoic acid, dichloromethane, 68%.

in Scheme 3 by TCFH mediated amide bond formation of **11a** with the corresponding aniline followed by boc-deprotection with TFA yielding piperidine **17** which was then reacted with 5-chloro-3-phenyl[1,2,4]oxadiazole. The alternative route to **18** via reaction of **17** with cyanogen bromide followed by ring closure with *N*-hydroxybenzamidine resulted in a lower total yield. Compared to **16**, **18** exhibited increased agonistic activity in terms of both potency ($EC_{50} = 30 \pm 11$ nM) and efficacy ($173 \pm 7\%$ IA).

We then considered combinations of promising LHS and RHS decorations, exemplified by spiro compound **21** (see Scheme 4). HATU assisted amide coupling followed by attachment of the phenyl substituted oxadiazole yielded **20** which was subsequently oxidized with *m*CPBA to give methanesulfonyl substituted **21**. **21** showed an EC_{50} of 21 ± 15 nM, while being a borderline full agonist with an intrinsic activity of $160 \pm 6\%$ IA.

The structure–activity relationships obtained from **21**, its close analogues, and other related potent and fully efficacious compounds with structurally diverse substitution patterns (compounds and data not shown) were very promising. Thus, we progressed 1-oxa-2,8-diaza-spiro[4.5]dec-2-ene type compounds into a lead optimization program with the goal to identify candidates for preclinical development in order to provide new options to treat type 2 diabetes mellitus.

SUMMARY AND CONCLUSION

The discovery of a novel lead class of GPR119 agonists was achieved through a fruitful combination of virtual screening and combinatorial chemistry using the BICLAIM approach. In our group we successfully applied this technology in various projects, yielding single hits, leads, or even advanced compound classes. The pillars for this success are diverse. First, our vast virtual BICLAIM space is based on numerous manifold combinatorial libraries. The chemistry to synthesize the libraries and their building blocks is well established in-house, allowing for short cycle times from idea to synthesis. Second, it is important to identify and select the most appropriate and promising scaffolds followed by a careful selection of their decoration. We noticed that the synthesis of virtual hits as combinatorial library arrays using a much more diverse decoration pattern than suggested by the single *in silico* hits dramatically increases the probability of discovering real hits. The design of these libraries is done as teamwork involving computational, combinatorial, and medicinal chemists, making extensive use of in-house and literature knowledge. In our

experience, the synthesis only of prototypic virtual hits as diagnostic compounds has turned out to be inferior. Third, the concept of an “activity anchor” has been proven rewarding and also increases the chances of finding true hits. We successfully applied the above-mentioned factors for the *in silico* discovery, selection, and design of two combinatorial libraries, which yielded two new structural classes of potent GPR119 agonists. Subsequent improvement of spiro compound **16** finally led to a new lead class.

EXPERIMENTAL SECTION

Virtual Screening. The query molecules were generated in ISIS Draw³⁸ and exported as mol files. Hydrogens and formal charges were added with Corina:³⁰

```
corina -i t=sdf -o t=mol2 -d wh -o fcharges input.mol
query.mol2
```

For the fragment space search with the FTrees software¹⁷ the following script was used:

```
ftrees
mol
convert query.mol2 1 1 query.fdf n y
ftrees
read 0 query.fdf
ftrees>fragspace
read BICLAIM.fsf y n
ftrees>ffsearch
mcreate 0 10 0.75 1.5
msearch 10000 y n
seloutput hits.smi
2smiles 1-10000 y y y s n
quit
```

The smiles files were converted to SD files, and the structures were unified using Pipeline Pilot.³⁹

For the postprocessing with ROCS²⁹ the following commands were used:

```
corina -i t=sdf -o t=sdf -d wh hits.sdf hits_3D.sdf
omega -in hits_3D.sdf -out hits_conf.oeb
rocs -query query.mol2 -dbase hits_conf.oeb -prefix
hits_aligned
```

The SD files resulting from ROCS²⁹ were imported in a MOE database and visually inspected with the database browser.²⁴

Determination of Agonistic Activity (hGPR119 Assay). The effect of the compounds on the activation of GPR119 and on the stimulation of intracellular cAMP concentration is determined using the ALPHAscreen cAMP assay kit (catalog no. 6760625R) made by PerkinElmer. MIN6 cells⁴⁰ are stably transfected with an expression vector for human GPR119 cDNA (accession no. NP_848566). Min-6/hGPR119 cells are cultured in DMEM, 10% FBS, 50 μ M β -mercaptoethanol, 0.6 mg/mL geneticin, 2 mM GlutaMAX at 37 °C, 5% CO₂. For the assay, the cells are seeded in culture plates (white, 384-well, TC, sterile with lid, catalog no. 6006280 (Perkin-Elmer); 10000 cells/well; 50 μ L). The plates covered with lids are then incubated for 24 h at 37 °C/5% CO₂. After the medium is aspirated from the wells completely, an amount of 10 μ L of the test compounds is added, the compounds are diluted using stimulating buffer (140 mM

NaCl, 3.6 mM KCl, 0.5 mM NaH₂PO₄, 0.5 mM MgSO₄, 1.5 mM CaCl₂, 10 mM Hepes, 5 mM NaHCO₃, pH 7.4, 0.5 mM IBMX, and 0.1% BSA; the final DMSO concentration is 1%). After 45 min of incubation at room temperature (approximately 20 °C), the cAMP concentrations are determined using the ALPHAscreen cAMP assay kit (catalog no. 6760625R from PerkinElmer). An amount of 10 μ L of biotin-cAMP-bead solution (final concentration of 1 U/well in lysing buffer (5 mM Hepes (pH 7.4), 0.1% BSA, 0.5% Tween)) is added. The plates are incubated for another 2 h at room temperature. The cAMP concentrations are calculated using a cAMP standard curve from the Alpha screen counts. The data analysis is carried out by calculating the EC₅₀ value and the maximum value based on a positive control (*N*-(4-methanesulfonylphenyl)-5-nitro-6-[4-(phenylsulfanyl)-piperidin-1-yl]pyrimidin-4-amine),³² using suitable software (XLfit). By default six measurements were conducted and the EC₅₀ was calculated using the geometric mean of the individual results (arithmetic mean for intrinsic activation).

Synthesis. All commercially available reagents were used without further purification unless otherwise stated. 3,9-Diaza-spiro[5.5]-undecane-3-carboxylic acid *tert*-butyl ester (**8a**, MFCD05861627) was purchased from Small Molecules, Inc., Hoboken, NJ, U.S. *tert*-Butyl 2,8-diaza-spiro[4.5]decane-8-carboxylate (**8b**, MFCD09608078), *tert*-butyl 2,7-diaza-spiro[3.5]nonane-2-carboxylate (**8c**, MFCD09834803), 8-(*tert*-butoxycarbonyl)-1-oxa-2,8-diaza-spiro[4.5]-dec-2-ene-3-carboxylic acid (**11a**, MFCD12198539), 7-(*tert*-butoxycarbonyl)-1-oxa-2,7-diaza-spiro[4.5]dec-2-ene-3-carboxylic acid (**11b**, MFCD12198540), and 7-(*tert*-butoxycarbonyl)-1-oxa-2,7-diaza-spiro[4.4]non-2-ene-3-carboxylic acid (**11c**, MFCD12198541) were purchased from WuXi App Tec Co. Ltd., Shanghai, China. ¹H NMR spectra were recorded on Bruker DRX 400 and DPX 400 spectrometers. Chemical shifts are reported in ppm using the residual of deuterated solvents as an internal standard. FTIR spectra were recorded using a Thermo Nicolet Avatar system 370. Prior to biological testing, NMR and/or analytical reversed phase HPLC was used to verify the purity of the compounds. All tested compounds derived from combinatorial libraries were at least 80% pure; all other compounds including resynthesis of the most interesting hits were at least 95% pure.

2,5-Difluoro-4-methylsulfanylphenylamine. 4-Bromo-2,5-difluorophenylamine (0.91 g, 4.4 mmol), CuI (120 mg, 0.63 mmol), NaI (1.31 g, 8.7 mmol), and dimethylethylenediamine (0.12 mL, 0.9 mmol) in 1,4-dioxane (4.0 mL) were purged with argon, and the mixture was stirred in a pressure pipe at 140 °C for 3 h. After the mixture was cooled to room temperature DCM was added, and the mixture was then washed consecutively with aqueous HCl solution (1 mol/L), aqueous Na₂CO₃ solution (10%), and brine. The organic layer was concentrated in vacuo to yield 2,5-difluoro-4-iodophenylamine (790 mg, 71%) which was used without further purification. Under an argon atmosphere 2,5-difluoro-4-iodophenylamine (790 mg, 3.1 mmol) was dissolved in dry DMF (4.0 mL), and dimethyl disulfide (0.68 mL, 7.7 mmol) was added followed by addition of NiBr₂ (80 mg, 0.37 mmol), 2,2-dipyridyl (50 mg, 0.32 mmol), and zinc dust (410 mg, 6.3 mmol). The reaction mixture was allowed to react at 80 °C for 2 h. After the mixture was cooled to room temperature DCM and active charcoal were added and the mixture was filtered through powdered cellulose. The remaining liquid is consecutively washed with aqueous Na₂CO₃ solution (10%) and brine. The organic layer was concentrated in vacuo to afford 2,5-difluoro-4-methylsulfanylphenylamine (400 mg, 74%) which was used without further purification. C₇H₇F₂NS (*M* = 175.2 g/mol). ESI-MS: 176 [M + H]⁺. *t*_R (HPLC): 1.09 min (Waters ZQ MS, Alliance 2690/2695, Waters XBridge C18 3.5 μ m, 4.6 mm \times 20 mm IS, flow 4.0 mL/min, temperature 40 °C, H₂O (+0.1% TFA)/MeOH).

General Procedure for the Synthesis of Spiro Ureas 9a–c (Library 1). To a stirred solution of amine **6** (0.10 mmol) in 1,4-dioxane (2.5 mL) were added sequentially DBU (30 μ L, 0.20 mmol) and CDT (7, 33 mg, 0.20 mmol). The mixture was stirred for 5 min at room temperature prior to addition of spiro-amine **8** (0.11 mmol) in 1,4-dioxane (1.0 mL). The reaction mixture was allowed to react at room temperature for 12 h. Subsequently the mixture was

concentrated in vacuo and the residue was purified by preparative reversed phase HPLC (C18 RP Sunfire column, gradient MeOH/H₂O (+0.1% TFA)) to afford the desired urea derivative.

9-(2-Bromo-4-methanesulfonylphenylcarbamoyl)-3,9-diazaspiro[5.5]undecane-3-carboxylic Acid *tert*-Butyl Ester (15).

Compound 15 was synthesized following the general procedure described above. 3,9-Diaza-spiro[5.5]undecane-3-carboxylic acid *tert*-butyl ester (8a) and 2-bromo-4-methanesulfonylphenylamine were used as starting materials. Yield: 21.5 mg (41%). C₂₂H₃₂BrN₃O₃S (*M* = 530.5 g/mol). ESI-MS: 530/532 [*M* + *H*]⁺. *t*_R (HPLC): 2.05 min (Agilent 1100 with DA and Waters MS detector, Sunfire C18, 4.6 mm × 50 mm, 3.5 μm (Waters), flow 1.5 mL/min, temperature 60 °C, H₂O (+0.1% TFA)/acetonitrile (+0.08% TFA)). ¹H NMR (400 MHz, DMSO-*d*₆): δ 1.38–1.43 (m, 4H), 1.39 (s, 9H), 1.45–1.50 (m, 4H), 3.24 (s, 3 H), 3.26–3.34 (m, 4H), 3.43–3.48 (m, 4H), 7.83 (dd, 1H, *J* = 8.6, 2.0 Hz), 7.88 (d, 1H, *J* = 8.6 Hz), 8.08 (d, 1H, *J* = 2.0 Hz), 8.24 (s, 1H).

General Procedure for the Synthesis of Spiro Amides 14a–c (Library 2). To a stirred solution of acid 11 (0.10 mmol) in THF (1.0 mL) were added sequentially DIPEA (52 μL, 0.30 mmol) and chloro-*N,N,N',N'*-tetramethylformamidinium hexafluorophosphate (TCFH 12, 45 mg, 0.16 mmol). The mixture was stirred for 45 min at room temperature prior to addition of a solution of the corresponding amine 13 (0.12 mmol) in THF (1.0 mL). The reaction mixture was allowed to react at room temperature for 12 h. Subsequently DMF was added and the mixture was filtered through basic aluminum oxide followed by washing with DMF/MeOH (9:1). The mixture was concentrated in vacuo, and the residue was taken up in DMF and was purified by preparative reversed phase HPLC (C18 RP Sunfire column, gradient MeOH/H₂O (+0.1% TFA)) to afford the desired amide.

3-(4-Cyano-2,5-difluorophenylcarbamoyl)-1-oxa-2,8-diazaspiro[4.5]dec-2-ene-8-carboxylic Acid *tert*-Butyl Ester (16). To a stirred solution of 8-(*tert*-butoxycarbonyl)-1-oxa-2,8-diazaspiro[4.5]dec-2-ene-3-carboxylic acid (11a, 150 mg, 0.53 mmol) in THF (3.0 mL) were added sequentially DIPEA (0.27 mL, 1.58 mmol) and chloro-*N,N,N',N'*-tetramethylformamidinium hexafluorophosphate (TCFH 12, 237 mg, 0.84 mmol). The mixture was stirred for 45 min at room temperature prior to addition of 4-amino-2,5-difluorobenzonitrile (89 mg, 0.60 mmol). The reaction mixture was allowed to react at room temperature for 12 h. The reaction mixture was quenched with water and was extracted with EtOAc. The combined organic layers were concentrated in vacuo. The residue was taken up in DMF and was purified by preparative reversed phase HPLC (C18 RP Sunfire column, gradient MeOH/H₂O (+0.1% TFA)) to afford compound 16 (73 mg, 33%). C₂₀H₂₂F₂N₄O₄ (*M* = 420.4 g/mol). ESI-MS: 421.2 [*M* + *H*]⁺. *t*_R (HPLC): 0.83 min (Waters Acquity with DA and MS detector, Sunfire C18, 2.1 mm × 50 mm, 2.5 μm (Waters), flow 1.5 mL/min, temperature 60 °C, H₂O (+0.1% formic acid)/acetonitrile (+0.1% formic acid)). ¹H NMR (400 MHz, DMSO-*d*₆): δ 1.41 (s, 9H), 1.71–1.77 (m, 4H), 3.11 (s, 2H), 3.35–3.47 (m, 4 H), 7.88–7.95 (m, 1H), 8.04–8.09 (m, 1H), 10.41 (s, 1H).

1-Oxa-2,8-diazaspiro[4.5]dec-2-ene-3-carboxylic Acid (4-Cyano-2,5-difluorophenyl)amide (17). To a stirred solution of 8-(*tert*-butoxycarbonyl)-1-oxa-2,8-diazaspiro[4.5]dec-2-ene-3-carboxylic acid (11a, 250 mg, 0.88 mmol) in DCM (40 mL) were added sequentially DIPEA (0.31 mL, 1.80 mmol) and chloro-*N,N,N',N'*-tetramethylformamidinium hexafluorophosphate (310 mg, 1.10 mmol). Subsequently 4-amino-2,5-difluorobenzonitrile (170 mg, 1.10 mmol) was added and the reaction mixture was allowed to react at room temperature for 7 days. The mixture was then washed consecutively with aqueous HCl solution (1 mol/L), aqueous Na₂CO₃ solution, and brine. The organic layer was treated with TFA (2 mL), and the mixture was stirred at room temperature for 2 h. The mixture was diluted with DCM, and aqueous HCl solution (50 mL, 1 mol/L) was added. To the aqueous layer was added DCM, and aqueous Na₂CO₃ solution was added until the mixture was basic. The organic layer was washed with brine followed by drying over Na₂SO₄ and concentration in vacuo to yield compound 17 (120 mg, 43%) as the corresponding hydrochloride, which was used without further

purification. C₁₅H₁₄F₂N₄O₂ (*M* = 320.3 g/mol). ESI-MS: 321 [*M* + *H*]⁺. *t*_R (HPLC): 0.93 min (Waters ZQ MS, Alliance 2690/2695, Waters XBridge C18 3.5 μm, 4.6 mm × 20 mm IS, flow 4.0 mL/min, temperature 40 °C, H₂O (+0.1% TFA)/MeOH). IR (ATR) *v*_{max} 3344, 2236, 1696, 1526, 1485, 1430, 1237, 909, 643 cm⁻¹. ¹H NMR (400 MHz, DMSO-*d*₆): δ 1.65–1.72 (m, 4H), 2.58–2.69 (m, 2H), 2.85–2.93 (m, 2H), 3.05 (s, 2H), 7.92–8.02 (m, 2H).

8-(3-Phenyl[1,2,4]oxadiazol-5-yl)-1-oxa-2,8-diazaspiro[4.5]dec-2-ene-3-carboxylic Acid (4-Cyano-2,5-difluorophenyl)amide (18). 17 (18 mg, 0.056 mmol) was dissolved in NMP (1.0 mL), and DIPEA (40 μL, 0.23 mmol) and 5-chloro-3-phenyl-1,2,4-oxadiazole (13 mg, 0.072 mmol) were added. The reaction mixture was allowed to react at 160 °C for 15 min. After the mixture was cooled to room temperature DCM was added and the mixture was washed consecutively with aqueous HCl solution (2 mol/L), aqueous Na₂CO₃ solution (10%), and brine. The organic layer was concentrated in vacuo, and the residue was purified by preparative MPLC (silica, DCM/MeOH = 98:2). The product containing fractions were concentrated in vacuo, and the residue was crystallized from diethyl ether/petrol ether to afford compound 18 (13 mg, 50%) as a colorless solid. C₂₃H₁₈F₂N₆O₃ (*M* = 464.4 g/mol). ESI-MS: 465 [*M* + *H*]⁺. *t*_R (HPLC): 1.52 min (Waters ZQ MS, Alliance 2690/2695, Waters XBridge C18 3.5 μm, 4.6 mm × 20 mm IS, flow 4.0 mL/min, temperature 40 °C, H₂O (+0.1% TFA)/MeOH). ¹H NMR (400 MHz, DMSO-*d*₆): δ 1.93–1.98 (m, 4H), 3.19 (s, 2H), 3.67–3.80 (m, 4H), 7.48–7.55 (m, 3H), 7.89–7.96 (m, 3H), 8.04–8.10 (m, 1H), 10.46 (s, 1H).

1-Oxa-2,8-diazaspiro[4.5]dec-2-ene-3-carboxylic Acid (2,5-Difluoro-4-methylsulfonylphenyl)amide (19). To a stirred solution of 8-(*tert*-butoxycarbonyl)-1-oxa-2,8-diazaspiro[4.5]dec-2-ene-3-carboxylic acid (11a, 600 mg, 2.11 mmol) in 1,2-dichloroethane (20 mL) were added sequentially DIPEA (0.65 mL, 3.780 mmol) and HATU (1.2 g, 3.2 mmol). The mixture was stirred at room temperature for 45 min. Subsequently 2,5-difluoro-4-methylsulfonylphenylamine (400 mg, 2.28 mmol) was added and the reaction mixture was allowed to react at room temperature for 3 h. The mixture was then washed consecutively with aqueous HCl solution (1 mol/L), aqueous Na₂CO₃ solution, and brine. The organic layer was concentrated and taken up in ethanol/DCM. In order to remove the boc protection group, the mixture was treated with ethereal HCl and the mixture was stirred at room temperature for 2 h. After completion of the reaction the precipitate was collected by filtration and was dried in vacuo to yield compound 19 (350 mg, 44%) as the corresponding HCl salt. C₁₅H₁₇F₂N₃O₂S·HCl (*M* = 377.8 g/mol). ESI-MS: 342 [*M* + *H*]⁺. *t*_R (HPLC): 1.13 min (Waters ZQ MS, Alliance 2690/2695, Waters XBridge C18 3.5 μm, 4.6 mm × 20 mm IS, flow 4.0 mL/min, temperature 40 °C, H₂O (+0.1% TFA)/MeOH). ¹H NMR (400 MHz, DMSO-*d*₆): δ 1.98–2.04 (m, 4H), 2.50 (s, 3H), 3.13–3.19 (m, 4H), 3.27 (s, 2H), 7.29–7.35 (m, 1H), 7.43–7.49 (m, 1H), 8.94 (bs, 2H), 10.16 (s, 1H).

8-(3-Phenyl[1,2,4]oxadiazol-5-yl)-1-oxa-2,8-diazaspiro[4.5]dec-2-ene-3-carboxylic Acid (2,5-Difluoro-4-methylsulfonylphenyl)amide (20). To a stirred solution of 19 (350 mg, 0.93 mmol) in NMP (5.0 mL) were added sequentially DIPEA (0.65 mL, 3.76 mmol) and 5-chloro-3-phenyl[1,2,4]oxadiazole (250 mg, 1.4 mmol). The mixture was stirred for 10 min at 150 °C. After cooling to room temperature, the reaction mixture was washed consecutively with aqueous HCl solution (2 mol/L), aqueous Na₂CO₃ solution (10%), and brine. The organic layer was concentrated under reduced pressure, and the residue was purified by MPLC (silica, DCM/MeOH = 97:3). The product containing fractions were concentrated in vacuo and the residue was crystallized from diethyl ether to afford compound 20 (230 mg, 51%) as a colorless solid. C₂₃H₂₁F₂N₅O₃S (*M* = 485.5 g/mol). ESI-MS: 486 [*M* + *H*]⁺. *t*_R (HPLC): 1.59 min (Waters ZQ MS, Alliance 2690/2695, Waters XBridge C18 3.5 μm, 4.6 mm × 20 mm IS, flow 4.0 mL/min, temperature 40 °C, H₂O (+0.1% TFA)/MeOH). ¹H NMR (400 MHz, DMSO-*d*₆): δ 1.92–1.98 (m, 4H), 2.51 (s, 3H), 3.17 (s, 2H), 3.71–3.77 (m, 4H), 7.30–7.36 (m, 1H), 7.45–7.55 (m, 4H), 7.89–7.93 (m, 2H), 10.16 (s, 1H).

8-(3-Phenyl[1,2,4]oxadiazol-5-yl)-1-oxa-2,8-diaza-spiro[4.5]-dec-2-ene-3-carboxylic Acid (2,5-Difluoro-4-methanesulfinylphenyl)amide (21). **20** (100 mg, 0.21 mmol) was dissolved in DCM (10 mL), and the mixture was cooled to 0 °C. 3-Chloroperoxybenzoic acid (38 mg, 0.22 mmol) was added, and the reaction mixture was allowed to react at 0 °C for 2 h. The mixture was then extracted with aqueous NaOH solution (1 mol/L), and the organic layer was washed with brine followed by drying over Na₂SO₄ and concentration in vacuo. The residue was triturated with diethyl ether, filtered, and dried to yield compound **21** (70 mg, 68%) as a colorless solid. C₂₃H₂₁F₂N₅O₄S (*M* = 501.5 g/mol). ESI-MS: 502 [M + H]⁺. *t*_R (HPLC): 1.44 min (Waters Alliance with DA and MS detector, Waters XBridge C18 3.5 μm, 4.6 mm × 30 mm, flow 4.0 mL/min, temperature 60 °C, H₂O (+0.1% TFA)/MeOH (+0.1% TFA)). ¹H NMR (400 MHz, DMSO-*d*₆): δ 1.94–1.99 (m, 4H), 2.87 (s, 3H), 3.19 (s, 2H), 3.71–3.78 (m, 4H), 7.49–7.55 (m, 3H), 7.56–7.61 (m, 1H), 7.72–7.77 (m, 1H), 7.89–7.93 (m, 2H), 10.38 (s, 1H).

AUTHOR INFORMATION

Corresponding Author

*Phone: +49-(0)7351-5494701. Fax: +49-(0)7351-8394701. E-mail: bernd.nosse@boehringer-ingenheim.com.

Notes

The authors declare no competing financial interest.

ACKNOWLEDGMENTS

The authors thank Georg Dahmann for assistance in the preparation of this manuscript. Additionally we thank Steffen Breitfelder, Peter Eickelmann, and Remko A. Bakker for valuable discussions and Angelika Raible-Pöschl as well as Esther Schmidt for biological activity measurements.

ABBREVIATIONS USED

cAMP, cyclic adenosine monophosphate; BICLAIM, Boehringer Ingelheim comprehensive library of accessible innovative molecules; CDT, 1,1'-carbonyldi(1,2,4-triazole); DBU, 1,8-diazabicyclo[5.4.0]undec-7-ene; DCM, dichloromethane; DIPEA, *N,N*-diisopropylethylamine; FBS, fragment based screening; FTrees, feature trees; GLP-1, glucagon-like peptide 1; GPR119, G-protein-coupled receptor 119; HATU, 2-(7-aza-1*H*-benzotriazole-1-yl)-1,1,3,3-tetramethyluronium hexafluorophosphate; HTS, high-throughput screening; LHS, left-hand side; NMP, *N*-methyl-2-pyrrolidinone; RHS, right-hand side; rt, room temperature; SAR, structure–activity-relationship; TCFH, chloro-*N,N,N',N'*-tetramethylformamidinium hexafluorophosphate; TFA, trifluoroacetic acid; THF, tetrahydrofuran; VS, virtual screening

REFERENCES

- (1) (a) Wild, S.; Roglic, G.; Green, A.; Sicree, R.; King, H. Global prevalence of diabetes: estimates for the year 2000 and projections for 2030. *Diabetes Care* **2004**, *27*, 1047–1053. (b) *Diabetes Atlas*, 2nd ed.; International Diabetes Federation: Brussels, Belgium, 2003. (c) International Diabetes Federation *Diabetes Atlas*. The Global Burden. <http://www.idf.org/diabetesatlas/Se/the-global-burden> (accessed September 2012).
- (2) Meece, J. Pancreatic islet dysfunction in type 2 diabetes: a rational target for incretin-based therapies. *Curr. Med. Res. Opin.* **2007**, *23*, 933–944.
- (3) Overton, H. A.; Babbs, A. J.; Doel, S. M.; Fyfe, M. C.; Gardner, L. S.; Griffin, G.; Jackson, H. C.; Procter, M. J.; Rasamison, C. M.; Tang-Christensen, M.; Widdowson, P. S.; Williams, G. M.; Reynet, C. Deorphanization of a G protein-coupled receptor for oleoylethanolamide and its use in the discovery of small-molecule hypophagic agents. *Cell Metab.* **2006**, *3*, 167–175.
- (4) Jones, R. M.; Leonard, J. N.; Buzard, D. J.; Lehmann, J. GPR119 agonists for the treatment of type 2 diabetes. *Expert Opin. Ther. Pat.* **2009**, *19*, 1339–1359.
- (5) Chu, Z.-L.; Carroll, C.; Chen, R.; Alfonso, J.; Gutierrez, V.; He, H.; Lucmn, A.; Xing, C.; Sebring, K.; Zhou, J.; Wagner, B.; Unett, D.; Jones, R. M.; Behan, D. P.; Leonard, J. *N*-Oleoyldopamine enhances glucose homeostasis through the activation of GPR119. *Mol. Endocrinol.* **2010**, *24*, 161–170.
- (6) Ezzili, C.; Otrubova, K.; Boger, D. L. Fatty acid amide signaling molecules. *Bioorg. Med. Chem.* **2010**, *20*, 5959–5968.
- (7) Ohishi, T.; Yoshida, S. The therapeutic potential of GPR119 agonists for type 2 diabetes. *Expert Opin. Invest. Drugs* **2012**, *21*, 321–328.
- (8) Semple, G.; Fioravanti, B.; Pereira, G.; Calderon, I.; Uy, J.; Choi, K.; Xiong, Y.; Ren, A.; Morgan, M.; Dave, V.; Thomsen, W.; Unett, D. J.; Xing, C.; Bossie, S.; Carroll, C.; Chu, Z.-L.; Grottick, A. J.; Hauser, E. K.; Leonard, J.; Jones, R. M. Discovery of the first potent and orally efficacious agonist of the orphan G-protein coupled receptor 119. *J. Med. Chem.* **2008**, *51*, 5172–5175.
- (9) Wu, Y.; Kuntz, J. D.; Carpenter, A. J.; Fang, J.; Sauls, H. R.; Gomez, D. J.; Ammal, C.; Xu, Y.; Hart, S.; Tadepalli, S. 2,5-Disubstituted pyridines as potent GPR 119 agonists. *Bioorg. Med. Chem. Lett.* **2010**, *20*, 2577–2581.
- (10) McClure, K. F.; Darout, E.; Guinaraes, C. R. W.; DeNinno, M. P.; Mascitti, V.; Munchhof, M. J.; Robinson, R. P.; Kohrt, J.; Harris, A. R.; Moore, D. E.; Li, B.; Samp, L.; Lefker, B. A.; Futatsugi, K.; Kung, D.; Bonon, P. D.; Cornelius, P.; Wang, R.; Salter, E.; Hornby, S.; Kalgutkar, A. S.; Chen, Y. Activation of the G-protein-coupled receptor 119: a conformation-based hypothesis for understanding agonist response. *J. Med. Chem.* **2011**, *54*, 1948–1952.
- (11) Semple, G.; Lehmann, J.; Wong, A.; Ren, A.; Bruce, M.; Shin, Y.-J.; Sage, C. R.; Morgan, M.; Chen, W.-C.; Sebring, K.; Chu, Z.-L.; Leonard, J.; A-Shamma, H.; Grottick, A. J.; Du, F.; Liang, Y.; Demarest, K.; Jones, R. M. Discovery of a second generation agonist of the orphan G-protein coupled receptor GPR119 with an improved profile. *Bioorg. Med. Chem. Lett.* **2012**, *22*, 1750–1755.
- (12) Negoro, K.; Yonetoku, Y.; Maruyama, T.; Yoshida, S.; Takeuchi, M.; Ohta, M. Synthesis and structure–activity relationship of 4-amino-2-phenylpyrimidine derivatives as a series of novel GPR119 agonists. *Bioorg. Med. Chem.* **2012**, *20*, 2369–2375.
- (13) Scott, J. S.; Birch, A. M.; Brocklehurst, K. J.; Broo, A.; Brown, H. S.; Butlin, R. J.; Clarke, D. S.; Davidsson, Ö.; Ertan, A.; Goldberg, K.; Groombridge, S. D.; Hudson, J. A.; Laber, D.; Leach, A. G.; MacFaul, P. A.; McKerrecher, D.; Pickup, A.; Schofield, P.; Svensson, P. H.; Sörme, P.; Teague, J. Use of small-molecule crystal structures to address solubility in a novel series of G protein coupled receptor 119 agonists: optimization of a lead and in vivo evaluation. *J. Med. Chem.* **2012**, *55*, 5361–5379.
- (14) Lessel, U.; Wellenzohn, B.; Lilienthal, M.; Claussen, H. Searching fragment spaces with feature trees. *J. Chem. Inf. Model.* **2009**, *49*, 270–279.
- (15) Boehm, M.; Wu, T.-Y.; Claussen, H.; Lemmen, C. Similarity searching and scaffold hopping in synthetically accessible combinatorial chemistry spaces. *J. Med. Chem.* **2008**, *51*, 2468–2480.
- (16) Rarey, M.; Dixon, J. S. Feature trees: a new similarity measure based on tree matching. *J. Comput.-Aided Mol. Des.* **1998**, *12*, 471–490.
- (17) *FTREES*, version 2.3.0; Biosolve IT GmbH; St. Augustine, FL, 2010.
- (18) Rarey, M.; Stahl, M. Similarity searching in large combinatorial chemistry spaces. *J. Comput.-Aided Mol. Des.* **2001**, *15*, 497–520.
- (19) Fischer, J. R.; Lessel, U.; Rarey, M. LoFT: Similarity-driven multiobjective focused library design. *J. Chem. Inf. Model.* **2009**, *50*, 1–21.
- (20) Fischer, J. R.; Lessel, U.; Rarey, M. Improving similarity-driven library design: customized matching and regio-selective feature trees. *J. Chem. Inf. Model.* **2011**, *51*, 2156–2163.
- (21) Lessel, U.; Wellenzohn, B.; Fischer, J. R.; Rarey, M. Design of combinatorial libraries for the exploration of virtual hits from fragment space searches with LoFT. *J. Chem. Inf. Model.* **2012**, *52*, 373–379.

- (22) Lauri, G.; Bartlett, P. A. CAVEAT: a program to facilitate the design of organic molecules. *J. Comput.-Aided Mol. Des.* **1994**, *8*, 51–66.
- (23) Maass, P.; Schulz-Gasch, T.; Stahl, M.; Rarey, M. ReCore: a fast and versatile method for scaffold hopping based on small molecule crystal structure conformations. *J. Chem. Inf. Model.* **2007**, *47*, 390–399.
- (24) *Molecular Operating Environment (MOE)*, version 2010.10; Chemical Computing Group Inc. (1010 Sherbooke St. West, Suite No. 910, Montreal, Quebec, Canada, H3A 2R7), 2010.
- (25) Jones, R. M.; Semple, G.; Xiong, Y.; Shin, Y.-J.; Ren, A. S.; Lehmann, J.; Fioravanti, B.; Bruce, M. A.; Choi, J.; Sun, K. Substituted Aryl and Heteroaryl Derivatives as Modulators of Metabolism and the Prophylaxis and Treatment of Disorders Related Thereto. WO-2005121121, 2005; Arena Pharmaceuticals, Inc.
- (26) Fevig, J. M.; Wacker, D. A. [6,6] and [6,7]-Bicyclic GPR119 G Protein-Coupled Receptor Agonists. WO-2008137435, 2008; Bristol-Myers Squibb Company.
- (27) Jones, R. M.; Lehmann, J. Modulators of Metabolism and the Treatment of Disorders Related Thereto. WO-2008005576, 2008; Arena Pharmaceuticals Inc.
- (28) Bradley, S. E.; Fyfe, M. C. T.; Bertram, L. S.; Gattrell, W.; Jeevaratnam, R. P.; Keily, J.; Procter, M. J.; Rasamison, C. M.; Rushworth, P. J.; Sambrook-Smith, C. P.; Stonehouse, D. F.; Swain, S. A.; Williams, G. M. GPCR Agonists. WO-2007003962, 2007; Prosidion Ltd.
- (29) ROCS, version 3.1.0; OpenEye Scientific Software, Inc.: Santa Fe, NM, 2010.
- (30) *Corina*, version 3.46; Molecular Networks GmbH: Erlangen, Germany, 2008.
- (31) *Omega*, version 2.4.3; OpenEye Scientific Software, Inc.: Santa Fe, NM, 2010.
- (32) Zhu, X.; Huang, D.; Lan, X.; Tang, C.; Zhu, Y.; Han, J.; Huang, W.; Qian, H. The first pharmacophore model for potent G protein-coupled receptor 119 agonist. *Eur. J. Med. Chem.* **2011**, *46*, 2901–2907.
- (33) Valeur, E.; Bradley, M. Amide bond formation: beyond the myth of coupling reagents. *Chem. Soc. Rev.* **2009**, *38*, 606–631.
- (34) Jones, R. M.; Semple, G.; Fioravanti, B.; Pereira, G.; Calderon, I.; Uy, J.; Duvvuri, K.; Choi, J. S. K.; Xiong, Y.; Dave, V. 1,2,3-Trisubstituted Aryl and Heteroaryl Derivatives as Modulators of Metabolism and the Prophylaxis and Treatment of Disorders Related Thereto Such as Diabetes and Hyperglycemia. WO-2004065380, 2004; Arena Pharmaceuticals Inc.
- (35) Buzard, D. J.; Lehmann, J.; Han, S.; Jones, R. M. GPR119 agonists 2009–2011. *Pharm. Pat. Anal.* **2012**, *1*, 285–299.
- (36) (a) Bertram, L. S.; Fyfe, M. C. T.; Jeevaratnam, R. P.; Keily, J.; Krulle, T. M.; Rasamison, C. M.; Sambrook-Smith, C. P.; Swain, S. A. Piperidinyl GPCR Agonists. WO-2010004343, 2010; Prosidion Limited. (b) Wood, H. B.; Szcwzyk, J. W.; Huang, Y.; Adams, A. D. Substituted Cyclopropyl Compounds, Compositions Containing Such Compounds and Methods of Treatment. WO-2009129036, 2009; Merck & Co. Inc. (c) Wood, H. B.; Adams, A. D.; Szcwzyk, J. W.; Zhang, Y.; Yang, M. Substituted Cyclopropyl Compounds, Compositions Containing Such Compounds and Methods of Treatment. WO-2011019538, 2011; Merck Sharp & Dohme Corp. (d) Birch, A. M.; Broo, D. A.; Butlin, R. J.; Clarke, D. S.; Davidsson, O. P.; De La Motte, H.; Johansson, K. E.; Leach, A.; Macfaul, P. A.; O'Donnell, C. J.; Scott, J. S.; Whittamore, P. R. O. 4-(Pyrimidin-2-yl)-piperazine and 4-(Pyrimidin-2-yl)-piperidine Derivatives as GPR119 Modulators. WO-2011030139, 2011; AstraZeneca UK Limited.
- (37) (a) Bertram, L. S.; Fyfe, M. C. T. Piperidinyl GPCR Agonists. WO-2010004345, 2010; Prosidion Limited. (b) Carpenter, A. J.; Fang, J.; Peckham, G. Chemical Compounds and Uses. WO-2010014593, 2010; Smithkline Beecham Corporation. (c) Barba, O.; Bell, J. C.; Dupree, T. B.; Fry, P. T.; Bertram, L. S.; Fyfe, M. C. T.; Gattrell, W.; Jeevaratnam, R. P.; Keily, J.; Krulle, T. M.; McDonald, R. W.; Morgan, T.; Rasamison, C. M.; Schofield, K. L.; Stewart, A. J. W.; Swain, S. A.; Withall, D. M. Cycloamino Derivatives as GPR119 Agonists. WO-2011147951, 2011; Prosidion Ltd.
- (38) *MDL ISIS/Draw*, version 2.5 SR 3; MDL Information Systems, Inc.: San Leandro, CA, 1990–2003.
- (39) *Pipeline Pilot*, version 8.0.1; Accelrys Software Inc.: San Diego, CA, 2010.
- (40) Miyazaki, J.; Araki, K.; Yamato, E.; Ikegami, H.; Asano, T.; Shibasaki, Y.; Oka, Y.; Yamamura, K. Establishment of a pancreatic beta cell line that retains glucose-inducible insulin secretion: special reference to expression of glucose transporter isoforms. *Endocrinology* **1990**, *127*, 126–132.